Analytical Pyrolysis Characteristics of Enzymatic/Mild Acidolysis Lignin (EMAL)

Tengfei Li,[a] Gaojin Lyu,[a,*] Haroon A. M. Saeed,[a,b] Yu Liu,[a,*] Yinglong Wu,[a] Guihua Yang,[a] and Lucian A. Lucia [a,c]

Fast pyrolysis is a promising method that is being investigated for application in the degradation of lignin into phenolic chemicals. In this study, enzymatic/mild acidolysis lignin (EMAL) isolated from eucalyptus (E-EMAL) and wheat straw (W-EMAL) were characterized by pyrolysis-gas chromatography/mass spectrometry. The results showed that the compositions and yields of the products were determined by the lignin type and pyrolysis temperature. The identified products from the E-EMAL and W-EMAL pyrolysis mainly included G-phenols such as 2-methoxy-4-vinylphenol and guaiacol, S-phenols such as syringol and 2,6-dimmethoxy-4-(2-propenyl)-phenol, and H-phenols such as phenol, 2-methylphenol, and 4-vinylphenol. The overall yield of these phenolics varied with the investigated conditions. The G- and S-phenols were the primary products during the E-EMAL pyrolysis, while more H-phenols were produced during the W-EMAL pyrolysis. A compromise mild pyrolysis temperature of 450 °C to 650 °C resulted in a high phenolics yield, while a temperature greater than 650 °C led to the production of more aromatic hydrocarbons.

Keywords: Lignin; Pyrolysis; Phenolic compounds; Py-GC/MS

Contact information: a: Key Lab of Pulp and Paper Science and Technology of the Ministry of Education, Qilu University of Technology (Shandong Academy of Sciences), Jinan 250353, Shandong, China; b: Center of Fibers, Papers and Recycling, Faculty of Industries Engineering and Technology, University of Gezira, Box 20, Wad Medani 79371, Sudan; c: Department of Forest Biomaterials, North Carolina State University, Box 8005, Raleigh, NC 27695-8005, USA;
** Corresponding author: gaojinlv@qlu.edu.cn; leoliuyu@163.com*

INTRODUCTION

Lignin is one of the three main components of plants, along with cellulose and hemicellulose, and is the most abundant renewable aromatic polymer on earth (Saeed *et al.* 2012; Amin *et al.* 2017; MacLellan *et al.* 2017). Many studies have shown that lignin is a biomolecular polymer that consists of three main benzoyl propane structural units (syringyl (S), guaiacyl (G), and p-hydroxyphenyl (H)) linked by a variety of carbon-carbon and carbon-oxygen bonds (Boeriu *et al.* 2004; Feofilova and Mysyakina 2016; Xie *et al.* 2017). Lignin not only provides plants with physical strength, but it also contributes a major recalcitrance of lignocellulose to the biodegradation and bioconversion of cell wall carbohydrates. Therefore, in many lignocellulosic biomass transformation technologies, lignin must be removed by pretreatment for the easier and more efficient use of the carbohydrates (Zoia *et al.* 2008; Zheng and Rehmann 2014; Graglia *et al.* 2015; Guo *et al.* 2016).

Because of its natural aromatic structure, lignin has been recognized as a promising material for producing aromatic chemicals (Sun *et al.* 1998; Thakur *et al.* 2014; Xu *et al.*

2014; Domínguez-Robles *et al.* 2017). A variety of conversion technologies have been investigated to produce aromatic compounds, such as hydrogenolysis, oxidation, and pyrolysis. Hydrogenolysis is a method of depolymerizing lignin by using hydrogen and a suitable catalyst, which is effective for obtaining phenolic compounds (Wikberg and Maunu 2004; Zakzeski *et al.* 2010; Laurichesse and Avérous 2014; Li *et al.* 2015). However, the hydrogenation depolymerization method is limited by severe reaction conditions such as a high temperature and pressure, high operating requirements, high costs of hydrogen and catalysts, *etc.* (Pan *et al.* 2016; Zhu *et al.* 2016; Xiao *et al.* 2017). Oxidative degradation is also an effective method for lignin depolymerization (Yang *et al.* 2017). Oxidants, such as oxygen and hydrogen peroxide, have been successfully applied during pulping and bleaching in the paper industry. Oxidation could effectively remove lignin from wood pulp under relatively mild reaction conditions and effectively destroy the lignin macromolecular structure, which results in phenolic compounds and organic acids. However, the yield of phenolic compounds from the oxidative depolymerization of lignin is relatively low, and the degradation products are mainly organic acids (Kalliola *et al.* 2015; Ma *et al.* 2015; Díaz-Urrutia *et al.* 2016). Pyrolysis is a promising method that is being studied in the degradation of lignin to convert it to high value-added products. Pyrolysis can degrade lignin at high temperatures in a very short time (< 2 s) in the absence of oxygen. The lignin thermal cracking products are mainly phenolic compounds, coke, and gas. The phenolic compounds can be further processed and used as high-quality chemicals, and the coke with a higher carbon content can be used as a heating agent and column skeleton in industrial applications (Guo *et al.* 2017; Kawamoto 2017; Rouches *et al.* 2017).

Pyrolysis-gas chromatography/mass spectrometry (Py-GC/MS) is a suitable method for evaluating the structural and pyrolysis characteristics of all kinds of polymer materials (Liu *et al.* 2016). Solid samples can be directly used in Py-GC/MS testing without pretreatment. The analysis of pyrolysis products not only assists in understanding the chemical structure of lignin, but more importantly, it helps to determine the distribution of lignin pyrolysis products under different thermochemical conditions (Guerra *et al.* 2008; Lou *et al.* 2010; Jiang *et al.* 2017).

Because of the complexity and difficulty of lignin separation, many studies have used industrial lignin as a raw material to investigate the thermal degradation properties of lignin. This is biased to a certain extent because the structure and thermal proprieties of lignin are mainly dependent on the separation methods and raw materials. Compared with industrial lignin, such as alkali lignin, kraft lignin, and other biorefinery lignins, enzymatic/mild acid hydrolysis lignin (EMAL) has more advantages, such as a high purity and yield. Moreover, its macromolecular structure is more intact than industrial and biorefinery lignins and closest to the structure of protolignin. Therefore, EMAL is more representative in the study of the pyrolysis mechanism and product distribution of lignin (Guo *et al.* 2016). Pyrolysis of EMAL isolated from non-wood plants such as bamboo, rice straw, sugarcane bagasse, and corn stalk *etc.* with a focus both on pyrolysis kinetics and on analysis of pyrolysis products have been extensively studied (Lou *et al.* 2010; Lv *et al.* 2010; Lv and Wu 2012; Lou *et al.* 2018). However, there has been little research on the pyrolysis of wood EMAL and its comparison with herbaceous EMAL.

In this study, the enzymatic/mild acid hydrolysis method was used to extract lignin from eucalyptus and wheat straw. The obtained eucalyptus enzymatic/mild acid hydrolysis lignin (E-EMAL) and wheat straw enzymatic/mild acid hydrolysis lignin (W-EMAL) were investigated in terms of their chemical structure, pyrolysis characteristics of natural

polymeric lignin, and product distribution *via* Fourier transform infrared spectrometry (FT-IR), thermogravimetric analysis (TGA), and Py-GC/MS.

EXPERIMENTAL

Materials

The eucalyptus was harvested and sawn in a forestry center in Zhuzhou, Hunan Province, China, and the wheat straw was harvested in Linyi, Shandong Province, China. The sample of the sawed eucalyptus trunk (leaves and bark excluded) had a length of 1 m and a diameter cross-section of 18 cm, and weighed approximately 18 kg. The wheat straw had an average length of 80 cm and was air-dried at ambient temperature in the lab for two months. The air-dried samples were cut and ranged from 2 cm to 4 cm in size, and then the samples were ground in a star mill (FW-102, Everbright, Beijing, China). The 40 mesh to 60 mesh fractions after acetone extraction for 48 h were used as the raw material for lignin separation. After the raw materials were dried in a vacuum oven (P_2O_5 as a desiccant) they were placed in a roller ball mill (F-P4000E, Focucy, Hunan, China) for 240 h at room temperature with a rotational speed of 36 rpm (Lou *et al.* 2010). The ball-milled raw materials were used for the preparation of EMAL after being subjected to benzene and ethanol extraction for 8 h.

Preparation of the EMAL

The raw materials were treated with highly active liquid cellulases (purified from *Trichoderma viride*, 8000 carboxymethyl cellulase activity units per mL of enzyme solution) that were purchased from Sinopharm Group Chemical Reagent Co., Ltd. (Shanghai, China), and the volume fraction of the enzyme solution was 10%. Enzymatic hydrolysis of the raw materials was performed for 48 h in a shaking table at a speed of 240 rpm, where the reaction temperature was 40 °C and the pH of the buffer solution was 4.5. The suspension was subjected to centrifugation after enzymolysis to obtain the enzymatically hydrolyzed crude lignin containing a small amount of carbohydrates. The isolated crude lignin was then washed with a dilute hydrochloric acid solution that had a pH of 2. The final crude lignin was freeze-dried.

The crude enzymatic lignin was dispersed in 100 mL of a dioxane-water mixture that contained 85 mL of dioxane and 15 mL of water, which was then refluxed at 87 °C under nitrogen for 2 h. After completion of the reaction, the mixture was filtered and the residue was washed with a neutral dioxane-water mixture to clarify the filtrate. The obtained filtrate was neutralized with sodium bicarbonate and concentrated under a reduced pressure at 35 °C. A small amount of concentrated solution was slowly added to a large amount of acidic deionized water. The mixture was centrifuged after standing for 12 h, and then the remaining solid was freeze-dried. The dried solid was purified with chromatographically pure n-hexane to remove the residual extract and then dried in a vacuum oven to yield a dry solid EMAL.

Methods

Elemental analysis

The carbon (C), nitrogen (N), hydrogen (H), and sulfur (S) contents (wt.%) in the EMAL samples were identified *via* elemental analyzer (Vario EL III, Elementar, Hesse, Germany). The oxygen (O) content was calculated by the difference.

FT-IR spectroscopy

The EMAL samples were characterized *via* FT-IR (ALPHA, Bruker, Karlsruhe, Germany). The dried samples were embedded in spectrally pure KBr pellets with concentrations of approximately 1 mg/100 mg KBr. All of the spectra were recorded in the absorption spectrum band over the range of 2000 cm^{-1} to 600 cm^{-1}.

Thermogravimetric analysis

The EMAL samples were characterized *via* thermogravimetric analyzer (TGA Q50, TA Instruments, New Castle, DE, USA). Approximately 5 mg of each sample were tested over a temperature range of 40 °C to 800 °C at a heating rate of 10 °C/min under an N_2 atmosphere.

Py-GC/MS analysis

The fast pyrolysis experiments were done in a JHP-3 model Curie point pyrolyzer (CDS 5200, CDS Analytical, Oxford, MS, USA) directly connected to a 7890B-5977A GC-MS (Agilent, Santa Clara, CA, USA). Approximately 0.1 mg of each sample was placed in a quartz tube, and the tubes were inserted into a pyroprobe for the pyrolysis experiments. The samples in the pyroprobe were heated at a certain temperature at a temperature ramp rate of 20 °C/ms with a final dwell time of 15 s. The gas products that were pyrolyzed were purged by high purity He (99.9995%) in the gas chromatograph. The valve oven and transfer lines were maintained at 250 °C and 270 °C, respectively.

Separation of the pyrolysis products was achieved on a HP-5MS capillary column (Agilent, Santa Clara, USA) that had the dimensions 30 m × 0.25 mm × 0.25 μm. The GC oven temperature was kept at 50 °C for 2 min, then heated from 50 °C to 270 °C at a rate of 10 °C/min, and the final temperature (270 °C) was maintained for 3 min. The injector temperature was set at 270 °C in the split mode, and the split ratio was 50:1 with a high purity He carrier gas flow rate of 1 mL/min. The mass detector was operated in the electron impact ionization mode (70 eV) over the mass range of 45 *m*/*z* to 500 *m*/*z*. The ion temperature and quadrupole temperature were set to 230 °C and 150 °C, respectively. The pyrolysis compounds were identified by comparing their corresponding mass spectral fragments with the NIST mass spectral library (NIST 14, U.S. Department of Commerce, Gaithersburg, MD, USA).

RESULTS AND DISCUSSION

Elemental Analysis

The elemental compositions of the W-EMAL and E-EMAL are listed in Table 1. Table 1 shows that both the W-EMAL and E-EMAL had relatively high C contents, *i.e.* 56.9% and 57.3%, respectively, which suggested that they have a high calorific value. Compared with the W-EMAL, the E-EMAL had a relatively high H content and low N content. It was intriguing that the difference between the O/C ratios of the W-EMAL and E-EMAL was small, but the H/C ratio of the E-EMAL was noticeably higher than that of the W-EMAL.

Table 1. Elemental Composition of the Lignin

Lignin Sample	Elemental Analysis (wt.%)					Element Molar Ratio	
	C	H	O	N	S	O/C	H/C
W-EMAL	56.9	5.0	37.2	0.9	0	0.5	1.1
E-EMAL	57.3	7.2	35.3	0.3	0	0.5	1.5

FT-IR Spectroscopy

The FT-IR spectra of the W-EMAL and E-EMAL are presented in Fig. 1, and the assignments of the FT-IR spectra in accordance with previous reports (Boeriu *et al.* 2004; Guo *et al.* 2015; Tong *et al.* 2017) are shown in Table 2. The bands located at 1600 cm^{-1} and 1510 cm^{-1} in the W-EMAL and E-EMAL indicated the presence of benzene rings in the lignin structures, which confirmed that they were seldom destroyed during the separation process. Additionally, the bands located at 1328 cm^{-1}, 1265 cm^{-1}, 1225 cm^{-1}, 1120 cm^{-1}, 1025 cm^{-1}, and 830 cm^{-1} indicated the existence of S and G units in the E-EMAL (Brebu *et al.* 2013). The higher intensity of the bands at 1328 cm^{-1} and 1225 cm^{-1} confirmed that S units played a dominant role in the E-EMAL. In contrast, lower intensity S units existed in the W-EMAL, which was indicated by the relatively weak bands at 1328 cm^{-1} and 1225 cm^{-1}. It was interesting that the bands at 1360 cm^{-1} and 1159 cm^{-1} were present in the W-EMAL because they suggested that H units were present. A small amount of carbohydrates was present in both lignins, which was indicated by the existence of the band at 1420 cm^{-1} (Xu *et al.* 2004; Zhang *et al.* 2012).

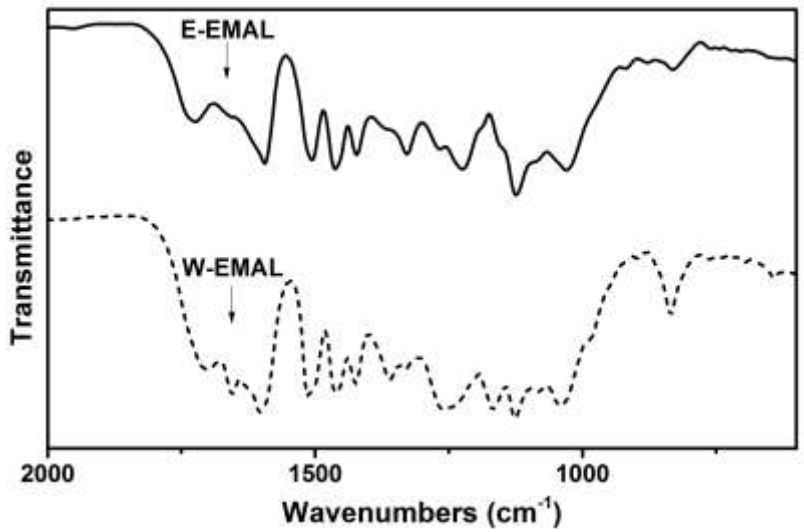

Fig. 1. FT-IR spectra of the E-EMAL and W-EMAL

Thermogravimetric Analysis

The TGA and derivative thermogravimetric (DTG) analysis curves of the W-EMAL and E-EMAL are shown in Fig. 2. The characteristic points (peak temperatures, maximum degradation rates, and residue solids) on the TGA and DTG curves of the W-EMAL and E-EMAL are listed in Table 3. Figure 2 shows that the mass loss of the two lignins mainly involved the evaporation of water when the temperature was less than 120 °C. The main lignin degradation occurred over the wide temperature range of 140 °C to 500 °C.

Table 2. Assignment of the FT-IR Spectra Bands of the W-EMAL and E-EMAL

Wavenumber (cm^{-1})	Assignment (Bond)	W-EMAL	E-EMAL
1712	C=O stretching vibration	1712	1712
1600, 1510	Aromatic ring skeleton vibration	1600, 1510	1600, 1510
1460	C-H deformation vibration in $-CH_2-$	1460	1460
1420	C-H bending vibration in $-CH_2-$ of cellulose	1420	1420
1360	O-H deformation vibration of phenol	1360	-
1328, 1225	C-O stretching vibration of syringyl units	-	1325, 1225
1265	C-O stretching vibration of guaiacyl units	1265	1265
1159	Coumaric acid ester	1159	-
1120, 830	C-H stretching vibration of syringyl units	1120	1120
1025	C-H bending vibration of guaiacyl units	1025	1025
915	C-H out-of-plane deformation of aromatic rings	915	915

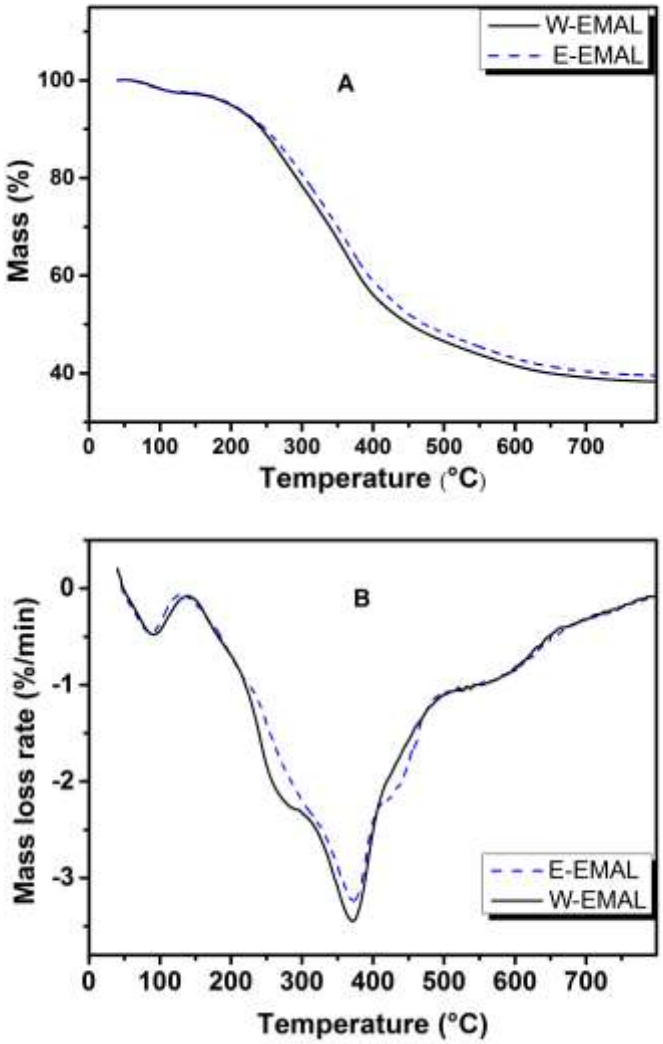

Fig. 2. TGA (A) and DTG (B) curves of the W-EMAL and E-EMAL at a heating rate of 10 °C/min

The degradation curves of the W-EMAL and E-EMAL almost coincided within the temperature range 140 °C to 220 °C. It was intriguing that the mass loss rate of the W-EMAL was relatively higher than that of the E-EMAL from 220 °C to 380 °C, and the maximum degradation rate of the W-EMAL was higher than that of the E-EMAL, which indicated that the degradation of the W-EMAL was more affected by the temperature. However, the difference in the peak temperature of the W-EMAL (372 °C) and E-EMAL (374 °C) was negligible, which suggested that the major chain linkages of the W-EMAL and E-EMAL were similar.

Table 3. Characterization of the Key Points of the TGA and DTG Curves of the W-EMAL and E-EMAL

Lignin	T_{max} [a] (°C)	MDR [b] (°C/min)	Residue Solids (%)
W-EMAL	372	3.5	38.3
E-EMAL	374	3.2	39.5
[a] Peak temperature of the DTG curve, which represents the maximum mass loss rate; [b] maximum degradation rate			

Table 4. Identified Products from the Pyrolysis of the W-EMAL and E-EMAL

Retention Time (min)	Compound	Relative Percentage (W (Area)/%)	
		E-EMAL	W-EMAL
		550 °C	550 °C
4.328	3-Furaldehyde	1.4	1.6
6.39/7.59	D-Limonene	1.7	0.5
6.848	Phenol	-	5.4
8.038	2-Methylphenol	-	0.4
8.388	*p*-cresol	-	3.8
8.603	Guaiacol	16.7	14.7
9.55/10.868	4-(2,5-Dihydro-3-methoxyphenol)-butylamine	0.5	1.6
9.83	4-Ethylphenol	-	2.2
10.209	2-Methoxy-5-methylphenol	6.5	-
10.224	Creosol	3.0	1.2
10.326	2, 5-Dimethyl-1, 4-benzenediol	6.5	1.1
10.699	4-Vinylphenol	-	17.2
11.367	2-Methyl-3-Phenylpropionaldehyde	1.7	-
11.472	4-Ethyl-2-methoxyphenol	8.3	4.7
11.987	2-Methoxy-4-vinylphenol	24.3	26.9
12.567	Syringol	13.7	8.8
14.548	Butylated hydroxytoluene	-	1.4
15.232	3-*tert*-Butyl-4-hydroxyanisole	4.7	1.3
16.742	2, 6-Dimethoxy-4-(2-propenyl)-phenol	6.8	5.7
18.541	Syringaldehyde	2.1	1.5
19.187	Methoxyeugenol	-	0.8
The pyrolysis experiment was done at 550 °C for 15 s with Py-GC/MS			

Results of the Py-GC/MS

Pyrolysis products of the EMAL

Based on the TGA, the W-EMAL and E-EMAL pyrolysis processes were performed at 550 °C for 15 s with Py-GC/MS. The identified pyrolysis products are shown in Table 4. Table 4 shows that the pyrolysis products of the W-EMAL and E-EMAL

contained high quantities of G- and S-phenols. Moreover, H-phenols, such as phenol, 2-methylphenol, and 4-vinylphenol, were present in the W-EMAL pyrolysis products, which was consistent with the results of the FT-IR analysis. These findings indicated that *p*-hydroxyphenyl structural units (H units) were present in the W-EMAL (Fig. 1). Thus, the effect of the lignin types on the composition and distribution of the pyrolysis products could be obtained from Table 4, where G- and S-type phenolic compounds were the predominant products of the E-EMAL, and the G/S peak area ratio was 2.2. The main G- and S-type products were 2-methylphenol, 4-ethyl-2-methoxyphenol, 2-methoxy-4-vinylphenol, 2-methoxy-5-methylphenol, syringol, and 2, 6-dimmethoxy-4-(2-propenyl)-phenol *etc.*, which resulted from the free-radical depolymerization/fragmentation reactions during lignin pyrolysis (Zakzeski *et al.* 2010; Xu *et al.* 2014). As was expected, the G-, S-, and H-type phenolic compounds were all detected in the pyrolysis products of the W-EMAL, and the G/S/H peak area ratio was 3.1:1:1.7. This means that more H-phenols were present in the pyrolysis products of the W-EMAL compared to that of E-EMAL. For example, in contrast with the E-EMAL, large amounts of 4-vinylphenol (17.2%) and phenol (5.4%) were formed during the pyrolysis of the W-EMAL. Interestingly, H-phenols obtained from W-EMAL pyrolysis in this work were even higher than that of alkaline lignin and kraft lignin from wheat straw (Lin *et al.* 2015). According to previous studies, EMAL isolated from wheat straw contains relatively rich *p*-hydroxyphenyl structure and vinyl ether substructure compared to hardwood lignin and other industrial lignin from wheat straw (Yang *et al.* 2011; Lin *et al.* 2015; Wen *et al.* 2015). As a result, pyrolysis of W-EMAL produced more H-type phenolic compounds. Additionally, a small amount of 3-furaldehyde was present in the pyrolysis products from both the W-EMAL and E-EMAL, which could be originated from the carbohydrate impurities in the isolated EMAL as reported by Lou *et al.* (2010).

Effect of the pyrolysis temperature on the product distribution

The influence of the pyrolysis temperature (350 °C, 450 °C, 550 °C, 650 °C, and 800 °C) on the composition and distribution of the W-EMAL and E-EMAL pyrolysis products was also studied. Figure 3 shows that the main pyrolysis products were divided into four categories: G-phenols, S-phenols, H-phenols, and aromatic hydrocarbons. The G- and S-phenols constituted a predominant proportion of the E-EMAL pyrolysis products, with maximum yields at 450 °C and 650 °C, respectively (Fig. 3B). The homolysis and concerted decomposition of C_β-O linkage in lignin macromolecules resulted in producing a large amount of G-phenols and S-phenols such as guaiacol, 2-methoxy-4-vinylphenol, and syringol *etc*. (Table 4). Nevertheless, those alkyls or alkoxylated phenols that with complex side chains may undergo secondary cracking at high temperatures to produce simpler aromatic compounds such as H-phenols or aromatic hydrocarbons (Lou *et al.* 2018; Liu *et al.* 2016). For example, at 350 °C, the yield of 2-methoxy-4-vinylphenol was highest, and then decreased as the temperature increased, which may because of its poorer thermal stability, with secondary pyrolysis occurring at elevated temperatures. The yields of the G- and S-phenols from the W-EMAL pyrolysis increased slowly and reached their highest levels at 450 °C and 650 °C, respectively. Moreover, the content of H-phenols from the W-EMAL pyrolysis increased as the temperature increase and reached its highest value at 800 °C (Fig. 3A). The H-phenols from W-EMAL pyrolysis was higher than that of E-EMAL, which was mainly because of more *p*-hydroxyphenyl (H-units) in herbaceous lignin (Lin *et al*. 2015). It was intriguing that aromatic hydrocarbons were detected during the pyrolysis of both W-EMAL and E-EMAL and remarkably increased when the pyrolysis

temperature was higher than 650 °C. This may have been because the lignin pyrolysis products produced at low temperatures were further degraded at high temperatures, and aromatic hydrocarbons, such as benzene and toluene, were formed (Brebu *et al.* 2013). It was concluded that the pyrolysis products depended strongly on both the origin of the lignin and pyrolysis temperature.

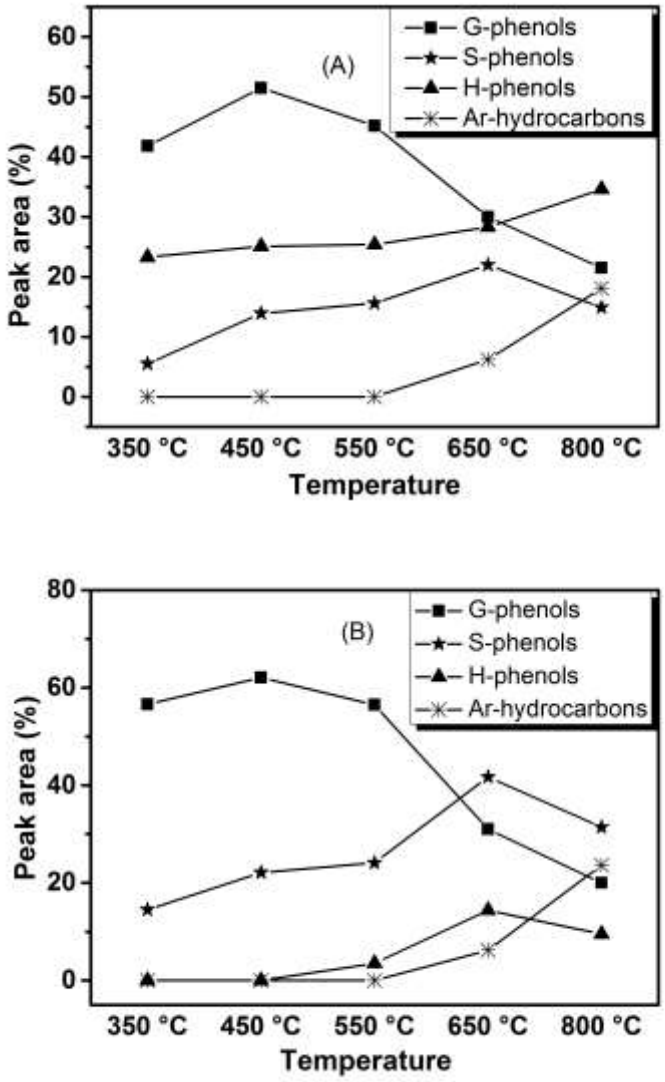

Fig. 3. Product distributions from the W-EMAL (A) and E-EMAL (B) pyrolysis at different temperatures

CONCLUSIONS

1. Both the origin of the lignin and pyrolysis temperature had a remarkable effect on the type and content of the pyrolysis products. The identified products from the E-EMAL and W-EMAL pyrolysis mainly included G-phenols such as 2-methoxy-4-vinylphenol and guaiacol, S-phenols such as syringol and 2, 6-dimmethoxy-4-(2-propenyl)-phenol, and H-phenols such as phenol, 2-methylphenol, *p*-cresol, and 4-vinylphenol.

2. The G- and S-phenols were the main E-EMAL pyrolysis products, and the maximum yields occurred at 450 °C and 650 °C, respectively. Compared with the E-EMAL, more H-phenols were formed during the pyrolysis of the W-EMAL, which reached its highest yield at 800 °C.
3. A compromise mild pyrolysis temperature ranging from 450 °C to 650 °C led to a high phenolics yield, while a temperature greater than 650 °C produced more aromatic hydrocarbons.

ACKNOWLEDGMENTS

The authors are grateful for the support of the National Key Research and Development Program of China (Grant No. 2017YFB0307900), the National Natural Science Foundation of China (Grant No. 31770630; 31770626), and the Taishan Scholars Program of Shandong Province.

REFERENCES CITED

Amin, F. R., Khalid, H., Zhang, H., Rahman, S. U., Zhang, R., Liu, G., and Chen, C. (2017). "Pretreatment methods of lignocellulosic biomass for anaerobic digestion," *AMB Express* 7(1), 72. DOI: 10.1186/s13568-017-0375-4

Boeriu, C. G., Bravo, D., Gosselink, R. J. A., and van Dam, J. E. G. (2004). "Characterisation of structure-dependent functional properties of lignin with infrared spectroscopy," *Ind. Crop. Prod.* 20(2), 205-218. DOI: 10.1016/j.indcrop.2004.04.022

Brebu, M., Tamminen, T., and Spiridon, I. (2013). "Thermal degradation of various lignins by TG-MS/FTIR and Py-GC-MS," *J. Anal. Appl. Pyrol.* 104, 531-539. DOI: 10.1016/j.jaap.2013.05.016

Díaz-Urrutia, C., Hurisso, B. B., Gauthier, P. M. P., Sedai, B., Singer, R. D., and Baker, R. T. (2016). "Catalytic aerobic oxidation of lignin-derived bio-oils using oxovanadium and copper complex catalysts and ionic liquids," *J. Mol. Catal. A-Chem.* 423, 414-422. DOI: 10.1016/j.molcata.2016.07.035

Domínguez-Robles, J., Sánchez, R., Espinosa, E., Savy, D., Mazzei, P., Piccolo, A., and Rodríguez, A. (2017). "Isolation and characterization of *Gramineae* and *Fabaceae* soda lignins," *Int. J. Mol. Sci.* 18(2), 327. DOI: 10.3390/ijms18020327

Feofilova, E., and Mysyakina, I. (2016). "Lignin: Chemical structure, biodegradation, and practical application (A review)," *Appl. Biochem. Micro.*+ 52(6), 573-581. DOI: 10.1134/S0003683816060053

Graglia, M., Kanna, N., and Esposito, D. (2015). "Lignin refinery: Towards the preparation of renewable aromatic building blocks," *ChemBioEng Reviews* 2(6), 377-392. DOI: 10.1002/cben.201500019

Guerra, A., Norambuena, M., Freer, J., and Argyropoulos, D. S. (2008). "Determination of arylglycerol−β-aryl ether linkages in enzymatic mild acidolysis lignins (EMAL): Comparison of DFRC/^{31}P NMR with thioacidolysis," *J. Nat. Prod.* 71(5), 836-841. DOI: 10.1021/np800080s

Guo, D., Wu, S., Lyu, G., and Guo, H. (2017). "Effect of molecular weight on the pyrolysis characteristics of alkali lignin," *Fuel* 193, 45-53. DOI:

10.1016/j.fuel.2016.12.042
Guo, T., Liu, Y., Liu, Y., Yang, G., Chen, J., and Lucia, L. A. (2016). "Chemical elucidation of structurally diverse willow lignins," *BioResources* 11(1), 2043-2054. DOI: 10.15376/biores.11.1.2043-2054
Guo, Y., Zhou, J., Wen, J., Sun, G., and Sun, Y. (2015). "Structural transformations of triploid of *Populus tomentosa* Carr. lignin during auto-catalyzed ethanol organosolv pretreatment," *Ind. Crop. Prod.* 76, 522-529. DOI: 10.1016/j.indcrop.2015.06.020
Jiang, X., Lu, Q., Hu, B., Liu, J., Dong, C., and Yang, Y. (2017). "A comprehensive study on pyrolysis mechanism of substituted β-O-4 type lignin dimers," *Int. J. Mol. Sci.* 18(11). DOI: 10.3390/ijms18112364
Kalliola, A., Vehmas, T., Liitiä, T., and Tamminen, T. (2015). "Alkali-O_2 oxidized lignin - A bio-based concrete plasticizer," *Ind. Crop. Prod.* 74, 150-157. DOI: 10.1016/j.indcrop.2015.04.056
Kawamoto, H. (2017). "Lignin pyrolysis reactions," *J. Wood Sci.* 63(2), 117-132. DOI: 10.1007/s10086-016-1606-z
Laurichesse, S., and Avérous, L. (2014). "Chemical modification of lignins: Towards biobased polymers," *Prog. Polym. Sci.* 39(7), 1266-1290. DOI: 10.1016/j.progpolymsci.2013.11.004
Li, C., Zhao, X., Wang, A., Huber, G.W., and Zhang, T. (2015). "Catalytic transformation of lignin for the production of chemicals and fuels," *Chem. Rev.* 115(21), 11559-11624. DOI: 10.1021/acs.chemrev.5b00155
Lin, X., Sui, S., Tan, S., Pittman, C., Sun, J., and Zhang, Z. (2015). "Fast pyrolysis of four lignins from different isolation processes using Py-GC/MS," *Energies* 8(12), 5107-5121. DOI: 10.3390/en8065107
Liu, Y., Liu, Y., Lyu, G., Ji, X., Yang, G., Chen, J., and Lucia, L. A. (2016). "Analytical pyrolysis pathways of guaiacyl glycerol-β-guaiacyl ether by Py-GC/MS," *BioResources* 11(3), 5816-5828. DOI: 10.15376/biores.11.3.5816-5828
Lou, R., Wu, S., and Lv, G. (2010). "Effect of conditions on fast pyrolysis of bamboo lignin," *J. Anal. Appl. Pyrol.* 89(2), 191-196. DOI: 10.1016/j.jaap.2010.08.007
Lou, R., Lyu, G., Wu, S., Zhang, B., Zhao, H., and Lucia, L. A. (2018). "Mechanistic investigation of rice straw lignin subunit bond cleavages and subsequent formation of monophenols," *ACS Sustainable Chem. Eng.* 6(1), 430-437. DOI: 10.1021/acssuschemeng.7b02688
Lv, G., Wu, S., Lou, R., and Yang, Q. (2010). "Analytical pyrolysis characteristics of enzymatic/mild acidolysis lignin from sugarcane bagasse," *Cellulose Chem. Technol.* 44(9), 335-342.
Lv, G., and Wu, S. (2012). "Analytical pyrolysis studies of corn stalk and its three main components by TG-MS and Py-GC/MS," *J. Anal. Appl. Pyrol*. 97, 11-18. DOI: dx.doi.org/10.1016/j.jaap.2012.04.010
Ma, R., Xu, Y., and Zhang, X. (2015). "Catalytic oxidation of biorefinery lignin to value-added chemicals to support sustainable biofuel production," *ChemSusChem* 8(1), 24-51. DOI: 10.1002/cssc.201402503
MacLellan, J., Chen, R., Yue, Z., Kraemer, R., Liu, Y., and Liao, W. (2017). "Effects of protein and lignin on cellulose and xylan anaylses of lignocellulosic biomass," *J. Integr. Agr.* 16(6), 1268-1275. DOI: 10.1016/S2095-3119(15)61142-X
Pan, G.-Y., Ma, Y.-L., Ma, X.-X., Sun, Y.-G., Lv, J.-M., and Zhang, J.-L. (2016). "Catalytic hydrogenation of corn stalk into polyol over Ni-W/MCM-41 catalyst," *Chem. Eng. J.* 299, 386-392. DOI: 10.1016/j.cej.2016.04.074

Rouches, E., Dignac, M.-F., Zhou, S., and Carrere, H. (2017). "Pyrolysis-GC-MS to assess the fungal pretreatment efficiency for wheat straw anaerobic digestion," *J. Anal. Appl. Pyrol.* 123, 409-418. DOI: 10.1016/j.jaap.2016.10.012

Saeed, A., Jahan, M. S., Li, H., Liu, Z., Ni, Y., and van Heiningen, A. (2012). "Mass balances of components dissolved in the pre-hydrolysis liquor of kraft-based dissolving pulp production process from Canadian hardwoods," *Biomass Bioenerg.* 39, 14-19. DOI: 10.1016/j.biombioe.2010.08.039

Sun, R., Mott, L., and Bolton, J. (1998). "Isolation and fractional characterization of ball-milled and enzyme lignins from oil palm trunk," *J. Agr. Food Chem.* 46(2), 718-723. DOI: 10.1021/jf9705532

Thakur, V. K., Thakur, M. K., Raghavan, P., and Kessler, M. R. (2014). "Progress in green polymer composites from lignin for multifunctional applications: A review," *ACS Sustain. Chem. Eng.* 2(5), 1072-1092. DOI: 10.1021/sc500087z

Tong, R., Wu, C., Zhao, C., and Yu, D. (2017). "Separation and structural characteristics of lignin in the prehydrolysis liquor of *Whangee* dissolving pulp," *BioResources* 12(4), 8217-8229. DOI: 10.15376/biores.12.4.8217-8229

Wen, J., Sun, S., Yuan, T., and Sun, R. (2015). "Structural elucidation of whole lignin from Eucalyptus based on preswelling and enzymatic hydrolysis," *Green Chem.* 17(3), 1589-1596. DOI: 10.1039/c4gc01889c

Wikberg, H., and Maunu, S. (2004). "Characterisation of thermally modified hard- and softwoods by ^{13}C CPMAS NMR," *Carbohyd. Polym.* 58(4), 461-466. DOI: 10.1016/j.carbpol.2004.08.008

Xiao, L.-P., Wang, S., Li, H., Li, Z., Shi, Z.-J., Xiao, L., Sun, R.-C., Fang, Y., and Song, G. (2017). "Catalytic hydrogenolysis of lignins into phenolic compounds over carbon nanotube supported molybdenum oxide," *ACS Catal.* 7(11), 7535-7542. DOI: 10.1021/acscatal.7b02563

Xie, S. X., Li, Q., Karki, P., Zhou, F., and Yuan, J. S. (2017). "Lignin as renewable and superior asphalt binder modifier," *ACS Sustain. Chem. Eng.* 5(4), 2817-2823. DOI: 10.1021/acssuschemeng.6b03064

Xu, C., Arancon, R. A. D., Labidi, J., and Luque, R. (2014). "Lignin depolymerisation strategies: Towards valuable chemicals and fuels," *Chem. Soc. Rev.* 43(22), 7485-7500. DOI: 10.1039/C4CS00235K

Xu, F., Sun, R.-C., Sun, X.-F., Geng, Z., Xiao, B., and Sun, J. (2004). "Analysis and characterization of acetylated sugarcane bagasse hemicelluloses," *Int. J. Polym. Anal. Ch.* 9(4), 229-244. DOI: 10.1080/10236660490920228

Yang, D., Huang, W., Qiu, X., Lou, H., and Qian, Y. (2017). "Modifying sulfomethylated alkali lignin by horseradish peroxidase to improve the dispersibility and conductivity of polyaniline," *Appl. Surf. Sci.* 426, 287-293. DOI: 10.1016/j.apsusc.2017.07.102

Yang, Q., Wu, S., Lou, R., and Lv, G. (2011). "Structural characterization of lignin from wheat straw," *Wood Sci. Technol.* 45(3), 419-431. 10.1007/s00226-010-0339-1

Zakzeski, J., Bruijnincx, P. C. A., Jongerius, A. L., and Weckhuysen, B. M. (2010). "The catalytic valorization of lignin for the production of renewable chemicals," *Chem. Rev.* 110(6), 3552-3599. DOI: 10.1021/cr900354u

Zhang, M., Li, L., Zheng, M., Wang, X., Ma, H., and Wang, K. (2012). "Effect of alkali pretreatment on cellulosic structural changes of corn stover," *Environ. Sci. Technol.* 35(6), 27-31. DOI: 10.3969/j.issn.1003-6504.2012.06.007

Zheng, J., and Rehmann, L. (2014). "Extrusion pretreatment of lignocellulosic biomass: A review," *Int. J. Mol. Sci.* 15(10), 18967-18984. DOI: 10.3390/ijms151018967

Zhu, G., Ouyang, X., Jiang, L., Zhu, Y., Jin, D., Pang, Y., and Qiu, X. (2016). "Effect of functional groups on hydrogenolysis of lignin model compounds," *Fuel Process. Technol.* 154, 132-138. DOI: 10.1016/j.fuproc.2016.08.023

Zoia, L., Orlandi, M., and Argyropoulos, D. S. (2008). "Microwave-assisted lignin isolation using the enzymatic mild acidolysis (EMAL) protocol," *J. Agr. Food Chem.* 56(21), 10115-10122. DOI: 10.1021/jf801955b

Article submitted: February 6, 2018; Peer review completed: April 9, 2018; Revised version received: April 25, 2018; Accepted: April 27, 2018; Published: May 1, 2018.
DOI: 10.15376/biores.13.2.4484-4496